CHAPTER 8 ACCELERATOR SHIELDING AND RADIOACTIVATION

TABLE OF CONTENTS

Article **Page**

PART 1 POLICIES AND PROCEDURES CONCERNING SHIELDING OF ACCELERATORS/BEAMLINES

811 Policy on Design Criteria

1. Radiological control performance is affected by human performance and engineered design features. This Manual primarily addresses the way people operate and use existing facilities and sites. In addition, the following radiological control design criteria are provided for new facilities and major modifications to existing facilities:

    a. Dose equivalent rates in areas of continuous occupancy shall be less than an average of 0.5 mrem/hr and as far below this as is reasonably achievable. Exposure rates for potential exposure to radiological workers in areas without continuous occupancy shall be ALARA and such that individuals do not receive more than 20% of the applicable limits as stated in Table 2-1.

    b. Discharges of radioactive liquid to the environment are covered by the provisions of DOE 5400.5 (Chapter 2 Section 1, and Chapter 3) and the concentrations should be kept as far below the groundwater discharge limit as possible.

    c. Contamination should be controlled by providing containment of radioactive material which has the potential for generating removable contamination.

    d. Efficiency of maintenance, decontamination, operations, and decommissioning should be maximized.

    e. Materials and components should be selected to minimize the radiological concerns.

    f. Provisions should be made for donning and removal of protective clothing and for personnel monitoring, when appropriate.

    g. Criteria for the conduct and review of shielding assessments are set forth in this chapter.

    h. Internal exposure should be avoided by the use of engineered controls such as ventilation, containment, and filtration systems, where practicable (see also Article 316).

i. Dose to members of the public from all DOE airborne emissions sources should be maintained as low as reasonably achievable (see also Chapter 11).

2. Facilities currently under construction should be evaluated and the above criteria applied where practicable.

3. Locating eating areas, office space, rest rooms, drinking fountains, showers and similar facilities and devices within radiological areas are strongly discouraged. Unless office space is essential to support radiological work, steps should be taken to preclude unnecessary occupancy.

4. The design of facilities where neutron radiation is anticipated should use a quality factor of 10 unless measurements or calculations can demonstrate that a different quality factor more adequately describes the radiation field as given in 10 CFR 835.2 and reproduced *verbatim* in Tables 8-1 and 8-2.

5. New or modified accelerator/beamline facilities should have a shielding assessment performed, as specified in Article 812. (Many reference documents have been generated over the years at Fermilab and elsewhere that describe accelerator shielding design and radioactivation. These may be incorporated by reference in the accelerator/beamline shielding assessments, and are subject to the review procedures described in Article 812.)

6. For purposes of this article, a modification to shielding which requires a shielding assessment under Article 812 is one that has the potential to permanently change the level of personnel protection provided by radiation shielding. Such modifications include those which result in a permanent change to the personnel access status of an area or those which result in modification of the "official" as-built drawings maintained by FESS (see Article 812).

7. Division/Section ES&H personnel should be intimately involved in the conceptual radiological design process, and the design must also be reviewed by the ES&H Section.

8. The appendices to this chapter give suggested guidance concerning the technical aspects of estimating radiation shielding.

812 Responsibilities for Configuration Control of Radiation Shielding

1. Division/Section Heads are responsible for accelerator/beamline operations and those of the associated experimental program. These responsibilities include the fulfillment of the program elements listed below. They shall:

a. Develop and maintain a comprehensive inventory of beamline shielding against ionizing radiation in the areas assigned to them by the Director, and assure that the shielding complies with provisions of this manual.

b. Conduct a shielding assessment when new experiments are installed or when new beamlines are commissioned. Such assessments shall also be conducted when beamline operating conditions change such that the official "as-built" drawings maintained by the Facilities Engineering Services Section (see below) must be changed, or if the operating conditions (available intensity, energy, or particle type, etc.) result in a change to the access conditions applicable to a given area.

(1) The shielding assessment shall be a written description which includes calculations and measurements of possible radiation exposures, radiation shielding, beam optics and other relevant information.

(2) The shielding assessment must document the circumstances and controls which serve to limit the intensity of the maximum beam loss and/or its duration.

(3) The assessment shall establish the occupancy status and radiological posting requirements of areas with respect to the posting criteria of Article 234, 236.

(4) The assessment shall be reviewed internally within the originating division/section (and within any other affected division/section) and approved in writing by the responsible division/section head(s). This review is to be documented.

(5) Modifications to shielding shall be reviewed by the Facilities Engineering Services Section for structural engineering impact. Changes to the original set of "as-built" drawings shall be coordinated with the Facilities Engineering Services Section (FESS).

(6) The assessment shall be submitted to the Senior Radiation Safety Officer for review in a timely manner prior to the conduct of the operations covered in the assessment.

(7) The shielding assessment documentation shall be maintained as "controlled documents" with copies filed in both the division/section office and in the ES&H Section Office.

c. Maintain shielding of beamlines in their area of responsibility and determine and document appropriate beam operating parameter limits required to meet ES&H requirements of this manual (the "safety envelope").

d. Coordinate these responsibilities in regions of interface between divisions and sections.

e. Control the placement of temporary shielding in accelerator/beamline enclosures by some or all of the following provisions:

(1) appropriate labeling of such shielding to prevent its inadvertent removal

(2) appropriate securing of such shielding to prevent its inadvertent removal

(3) appropriate procedures for evaluating its effectiveness, and

(4) appropriate documentation which becomes part of the permanent record of the operation.

f. Implement procedures to assure proper review and control of temporary modifications to permanent shielding that do not meet the criteria of 1.b.

2. The Senior Radiation Safety Officer shall:

a. Review the shielding assessment and, if appropriate, recommend written approval by the Director.

b. Maintain records of such reviews including file copies of the "as-built" shielding documents and the shielding assessment documentation and review protocols.

3. The Head of the Facilities Engineering Services Section shall prepare and maintain the original set of "as-built" drawings documenting the status of radiation shielding. These drawings shall be approved by the appropriate division/section, the Senior Radiation Safety Officer, and the Director by signature. Thereafter Facilities Engineering Services will maintain the up-to-date originals of these drawings (and retain archival drawings of past conditions) while the ES&H Section and the appropriate division/section will be supplied up-to-date copies of the current shielding conditions.

Table 8-1 Quality Factors

The quality factors to be used for determining dose equivalent in rem are shown below:

Radiation Type	**Quality Factor**
X-rays, gamma rays, positrons, electrons (including H-3) beta particles)	1
Neutrons $\leq$ 10 keV	3
Neutrons > 10 keV	10
Protons and singly-charged particles of unknown energy with rest mass greater than one atomic mass unit	10
Alpha particles and multiple-charged particles (and particles of unknown charge) of unknown energy	20

Note: If the spectral data are insufficient to identify the energy of the neutrons, a quality factor of 10 shall be used. Should one be able to determine the energy of the neutrons more exactly, the following quality factors may be used in determining the dose equivalent.

Table 8-2 Neutron Quality Factors

Mean quality factors, QF (maximum value in a 30-cm dosimetry phantom), and values of neutron flux density that deliver in 40 hours a maximum dose equivalent of 100 mrem (0.001 sievert).

Neutron Energy (MeV)	**Mean QF**	**Neutron Flux ($cm^{-2}s^{-1}$)**	**Neutron Energy (MeV)**	**Mean QF**	**Neutron Flux ($cm^{-2}s^{-1}$)**
2.5×10^{-8} (thermal)	2	680	5	8	16
1×10^{-7}	2	680	7	7	17
1×10^{-6}	2	560	10	6.5	17
1×10^{-5}	2	560	14	7.5	12
1×10^{-4}	2	580	20	8	11
1×10^{-3}	2	680	40	7	10
1×10^{-2}	2.5	700	60	5.5	11
1×10^{-1}	7.5	115	1×10^{2}	4	14
5×10^{-1}	11	27	2×10^{2}	3.5	13
1	11	19	3×10^{2}	3.5	11
2.5	9	20	4×10^{2}	3.5	10

Appendix 8A Brief Summary Of General Methods Of Estimating Shielding and Radioactivation

1. Introduction

There are three principal reasons why accelerator and beamline components are shielded for radiation protection purposes:

A) to reduce the dose received by personnel during beam-on conditions;

B) to reduce exposure to personnel from highly radioactive targets and beam absorbers, etc.; and

C) to prevent contamination of the environment by creation of radioactivity in uncontrolled locations (see Chapter 11).

At a hadron accelerator, in particular, the design of adequate shielding becomes more complex with increasing beam energy. This is the result of the development of the internuclear cascade that can be described as follows: A high-energy hadron interacting with a nucleus typically creates a rather large number of short-lived particles (pions, kaons, etc.), as well as protons, neutrons and nuclear fragments. The more energetic of these particles may in turn interact with another nucleus and thereby create still more particles. This type of event or series of events is called a hadronic cascade or shower. Another result of high-energy hadron interactions is the production of muons. These particles, which behave in matter much like heavy electrons, represent a significant shielding problem at high energy accelerators. The interactions of the high energy beams can also produce significant radioactivation of the beamline components and the surrounding environment.

It is not the purpose of this Appendix to describe all aspects of radiation physics at accelerators. Indeed, this topic has been described elsewhere in generally available references (e.g., Co99, Pa73, Sc90, Su92). Such references should be consulted for detailed work. The purpose of the appendix is limited in scope to the summarization of the important features as a way of providing a convenient "ready-reference". For specific situations, individualized calculations should be performed as appropriate in accordance with FESHM Chapter 5201, "Usage of Computer Calculations Affecting Environment, Safety, and Health."

2. Prompt Radiation Shielding-Hadrons

A) Bulk Shielding

To correctly predict the behavior of the cascades in different materials arranged in an irregular geometry one must rely on computer programs that, to varying degrees, simulate these processes numerically (Monte-Carlo method). Historically, the code CASIM has been the main tool for doing such shielding calculations at Fermilab (Va75, Va87). Results obtained using this code still provide a benchmark for calculations of this type. More recently, the code MARS (Kr97) has supplanted CASIM as the code of choice for evaluating the shielding design of new projects. These codes use statistical techniques to "follow" through the shield the particles produced due to the incidence of primary protons. Various quantities are tabulated by location within the shield, generally by collecting them in geometrical bins specified by the program. The geometry of the shield is specifically incorporated into the calculation in accordance with the conventions of the program to the level of accuracy deemed appropriate by the user.

Collections of "standard", idealized calculations using such codes have been produced (Va75, Sc90, Va87, Co82a) that are helpful for evaluating commonly occurring situations. Further, the codes have been compared with each other, with results obtained with other codes used worldwide, and with experimental results (Aw75, Aw76, Co82a, Co82b, Co85, Mo86, Eb88, Su98, Sc90). Such "benchmarking" is being done on a continuing basis. The general agreement with measurement is excellent for situations in which the shield configuration and beam loss conditions are well-understood and where the calculations are carried out with an appropriate statistical precision.

The primary output of calculations of this type is “star” (i.e., nuclear interaction) densities (stars/(cm^3·incident proton) above a specified threshold momentum as a function of location in the thick shield. These locations will generally be associated with the geometrical bins mentioned above. In the past, a threshold momentum of 300 MeV/c (47 MeV kinetic energy for nucleons) has customarily been used as this value is generally above the domain of energy where nuclear structure resonance are important. Figures 8-1 and 8-2 are useful examples that show contours of star density in large solid iron and concrete shields for protons of 300 GeV/c incident momentum. Figure 8-3 is an idealization of a 300 GeV/c proton beam being lost on a magnet or collimator inside a tunnel. Figures 8-4 and 8-5 are similar to figures 8-1 and 8-2 except that they are for 1000 GeV/c incident protons.

The star density can be converted to dose equivalent and other quantities of radiobiological interest. Because the cascade propagates mainly forward (along the beam) and radially outward, one can generally assume that the material at larger depths or at larger radii does not influence the dose at the point of interest.

(i.e., The stars "shine" mainly in the direction of the particle creating the star.) The conversion factors relating star density to dose equivalent depends upon the momentum threshold assumed in the calculation, since particles below threshold can contribute to the dose, but not to the star density, and this contribution has to be included. There is a dependence of the conversion factors upon location in a shield. However, at sufficiently large depths or radii when the shape of the hadron spectrum approaches equilibrium they approach constant values.

Iron is sometimes used as part of hadron shielding at accelerators in order to minimize the space required for the shield by taking advantage of the higher density of iron relative to soil or concrete. To do this, one must be aware of a special physical effect. In the case of an all-iron (or any other non-hydrogenous material) shield, the shape of the spectrum changes dramatically with radius. At small radii (~10 cm) the spectrum is roughly 1/E. At larger radii, an increasing fraction of the neutrons have energies below several hundred keV. This phenomenon occurs in part because the first excited state in the nuclei of the stable iron isotopes is of the order of 800 keV so that the inelastic cross section for neutrons with energies below 1 MeV in the iron region is very small. The greater the radius of the iron shield, the more pronounced the excess of these intermediate over high-energy neutrons becomes. The spectrum appears to reach equilibrium for radii greater than a meter (Go76a). This phenomena has been verified experimentally (El86). Calculations have indicated that an outer layer of 60-90 cm of concrete will compensate for this effect and allows one to utilize the higher density of iron shields to optimize the space required for shielding (Yu83).

Table 8-1 gives quantities of interest for four spectra: a "thin" iron shield (r = 20 cm) (Go76a) in which the high-energy particles still play a significant role; a "thick" iron shield (r ≈ 100 cm) in which the spectrum is totally dominated by intermediate energy neutrons (El86), and the more familiar spectra found outside soil and concrete shields (El86). The results are a composite of those obtained using several different references cited. They include the contribution of the components of the neutron energy spectra that are below the "traditional" Monte-Carlo threshold of approximately 300 MeV/c. These quantities should be calculated directly for individual shielding/beam configurations wherever it is practical to do so. Other results of measurements in accelerator neutron spectra at Fermilab are provided elsewhere (Co88, Co99).

Soil is generally considered to be equivalent to concrete in hadron shielding problems, provided one scales all dimensions to compensate for the lesser density of soil. One unit linear thickness (i.e., ft or cm) of soil is approximately equivalent (41.6/44.6) = 0.93 unit thickness of concrete where the multiplicative factor is the ratio of the high energy interaction lengths provided in Table 8-1. The density of compacted soil is quite high at Fermilab (2.24 g cm^{-3}) compared with the uncompacted value of about 2.0 g cm^{-3} (Mu83).

Table 8-1

Shielding and neutron spectral quantities of interest for four side-shield spectra produced by multi-hundred GeV protons. See original references for more details. Here *t* denotes the approximate thickness of the material. The "thin" iron is the layer struck by primary protons or first generation secondary hadrons. For general purposes, a "thick" shield can be considered to be one that is thicker than approximately 1 interaction length.

Spectrum	**Iron "Thin" $t < 20$ cm (Go76a)**	**Iron "Thick" $t \approx 100$ cm (El86)**	**Concrete "Thick" $t \approx 100$ cm (El86)**	**Compacted Soil "Thick" (Inferred from El86)**
Density ρ (g cm^{-3})	7.87	7.86	2.4	2.24
Absorption Length (cm) (gm cm^{-2})	16.8 131.9	16.8 131.9	41.6 99.9	44.6 99.9
Average Quality Factor (Note 1)	7.7	5.7	2.7	2.7
Absorbed Dose/Neutron Fluence (mrad/n-cm^{-2})	2.4×10^{-6}	1.7×10^{-6}	5.7×10^{-7}	5.7×10^{-7}
Dose-Equivalent/Neutron Fluence (mrem/n-cm^{-2})	1.9×10^{-5}	9.5×10^{-6}	1.6×10^{-6}	1.6×10^{-6}
Neutron Fluence/star-cm^{-3} (n-cm^{-2}/Star-cm^{-3})	526	44200	3060	3310
Absorbed Dose/star-cm^{-3} (mrad/star-cm^{-3}) (Note 2)	1.3×10^{-3}	7.4×10^{-2}	1.8×10^{-3}	2.0×10^{-3}
Dose Equivalent/star-cm^{-3} (mrem/star-cm^{-3}) (Note 2)	1.0×10^{-2}	0.42	4.9×10^{-3}	5.3×10^{-3}

Notes:

1. These are values from a well-measured or well-calculated spectra. See other references for alternative examples of spectra. For example, quality factors from (Co88) for "thick iron" spectra range from 5.7 to 6.9 and for "concrete" from 2.5-5.8. Thus, one reasonably takes the value of QF ≈ 5 for "typical" neutron spectra when spectrum measurements are not available.
2. The values for concrete are adapted from (St86).

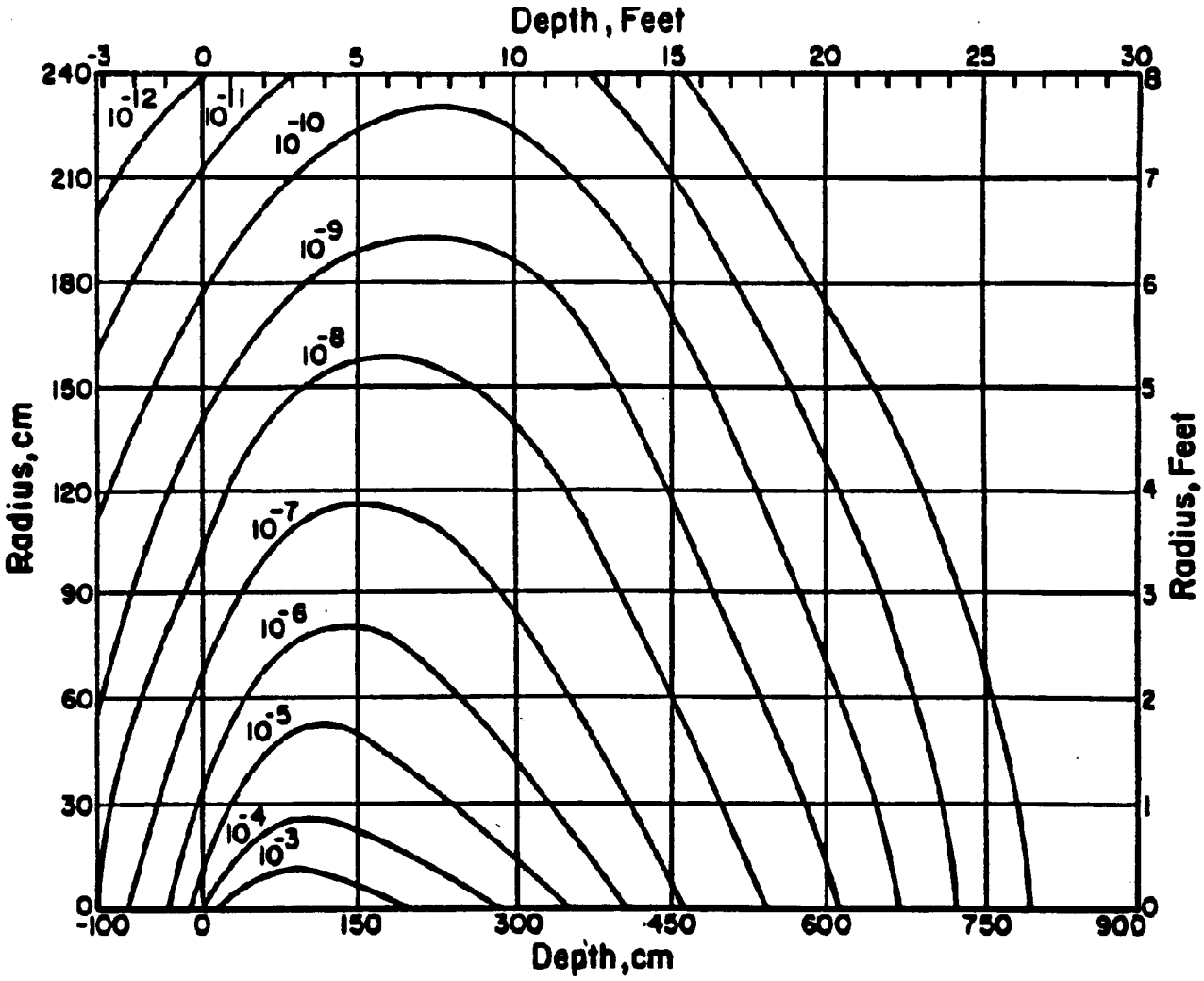

FIGURE 8-1

300 GeV/c protons incident on a solid iron cylinder. Contours of star density (stars cm^{-3} per incident proton) based on a CASIM simulation. The beam of 0.3 x 0.3 cm cross section is centered on the cylinder axis and starts to interact at zero depth. The star density includes only those due to hadrons above 0.3 GeV/c momentum. Contours of higher star density are not shown for clarity of the plot; those of lower star density are not included due to statistical uncertainty. (Fig. VIII.3 of Va75)

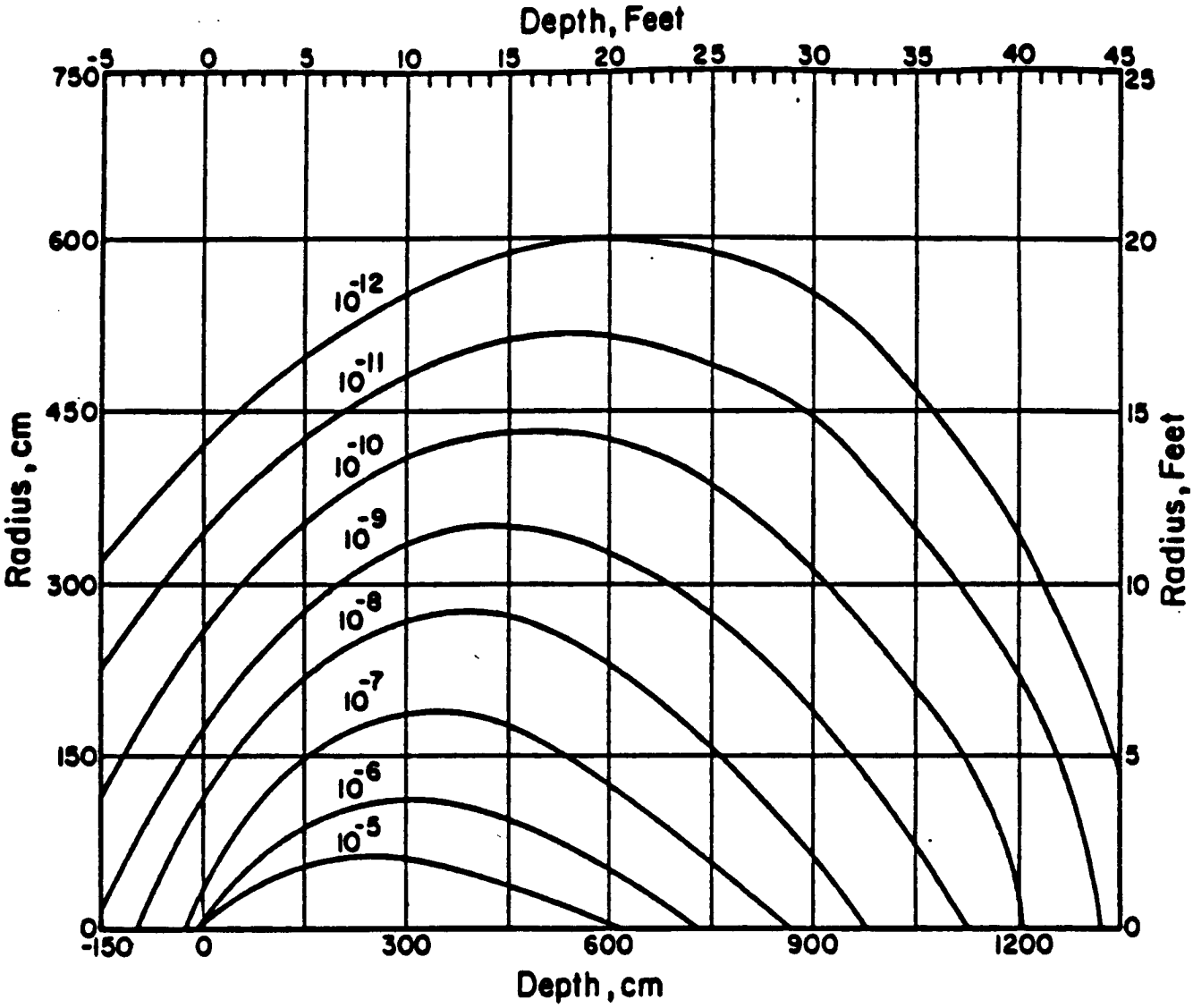

FIGURE 8-2

300 GeV/c protons incident on a solid concrete cylinder. Contours of star density (stars cm^{-3} per incident proton) based on a CASIM simulation. The beam of 0.3 x 0.3 cm cross section is centered on the cylinder axis and starts to interact at zero depth. The star density includes only those due to hadrons above 0.3 GeV/c momentum. Contours of higher star density are not shown for clarity of the plot; those of lower star density are not included due to statistical uncertainty. (Fig. VIII.20 of Va75)

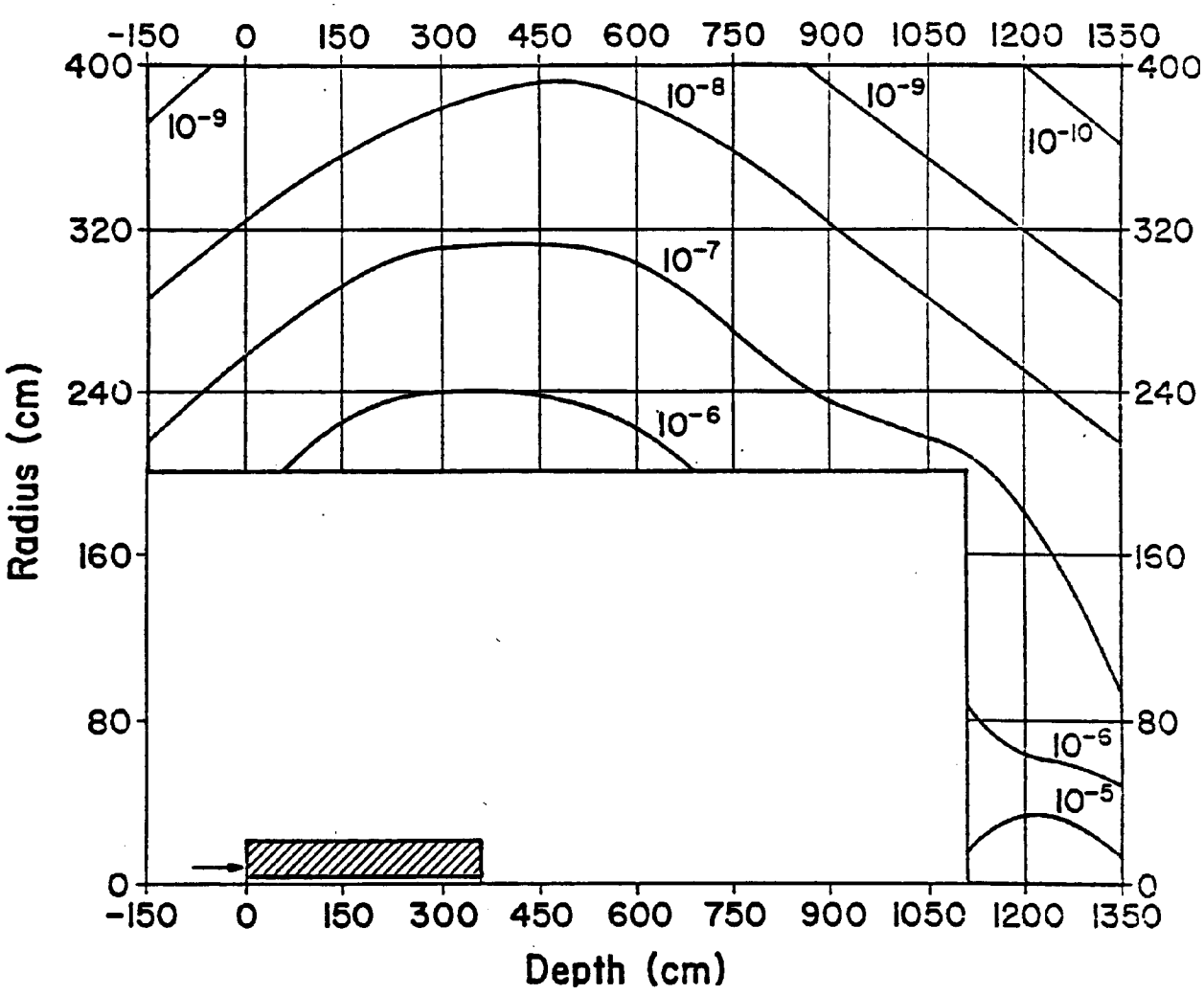

FIGURE 8-3

300 GeV protons incident on a steel "collimator" (or magnet) placed in a concrete enclosure based on a CASIM simulation. Contours of star density (stars cm^{-3} per incident proton) produced by hadrons above 0.3 GeV/c momentum. The collimator is a cylindrical shell, 360 cm long, with an outer radius of 20 cm and an inner radius of 3.75 cm. The beam has a square cross section of 0.1 x 0.1 cm and is centered at a radius of 4 cm. The contours show the star density averaged over azimuthal angle.

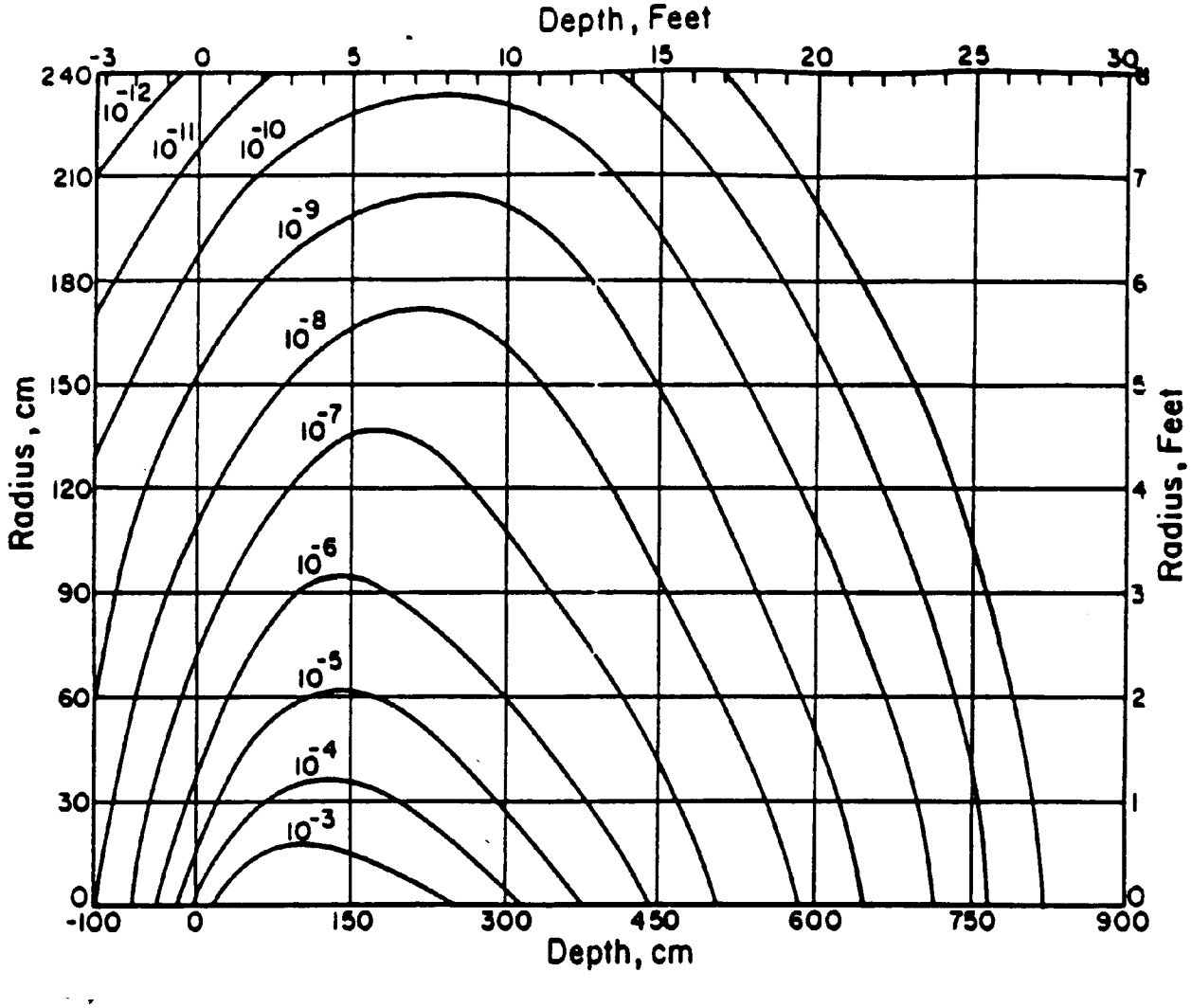

FIGURE 8-4

1000 GeV/c protons incident on a solid iron cylinder. Contours of star density (stars cm^{-3} per incident proton) based on a CASIM simulation. The beam of 0.3 x 0.3 cm cross section is centered on the cylinder axis and starts to interact at zero depth. The star density includes only those due to hadrons above 0.3 GeV/c momentum. Contours of higher star density are not shown for clarity of the plot; those of lower star density are not included due to statistical uncertainty. (Fig. VIII.4 of Va75)

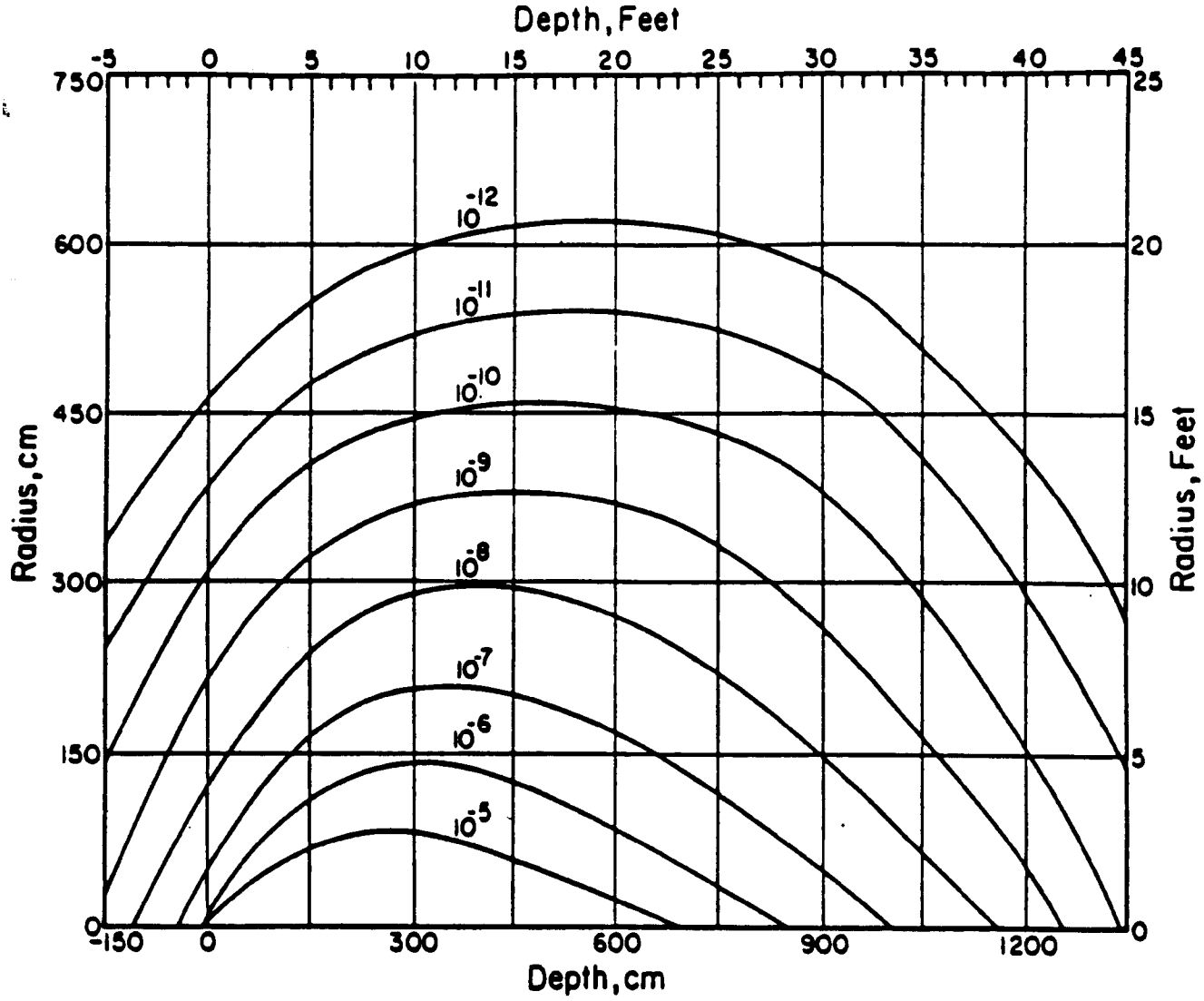

FIGURE 8-5

1000 GeV/c protons incident on a solid concrete cylinder. Contours of star density (stars cm^{-3} per incident proton) based on a CASIM simulation. The beam of 0.3 x 0.3 cm cross section is centered on the cylinder axis and starts to interact at zero depth. The star density includes only those due to hadrons above 0.3 GeV/c momentum. Contours of higher star density are not shown for clarity of the plot; those of lower star density are not included due to statistical uncertainty. (Fig. VIII.21 of Va75)

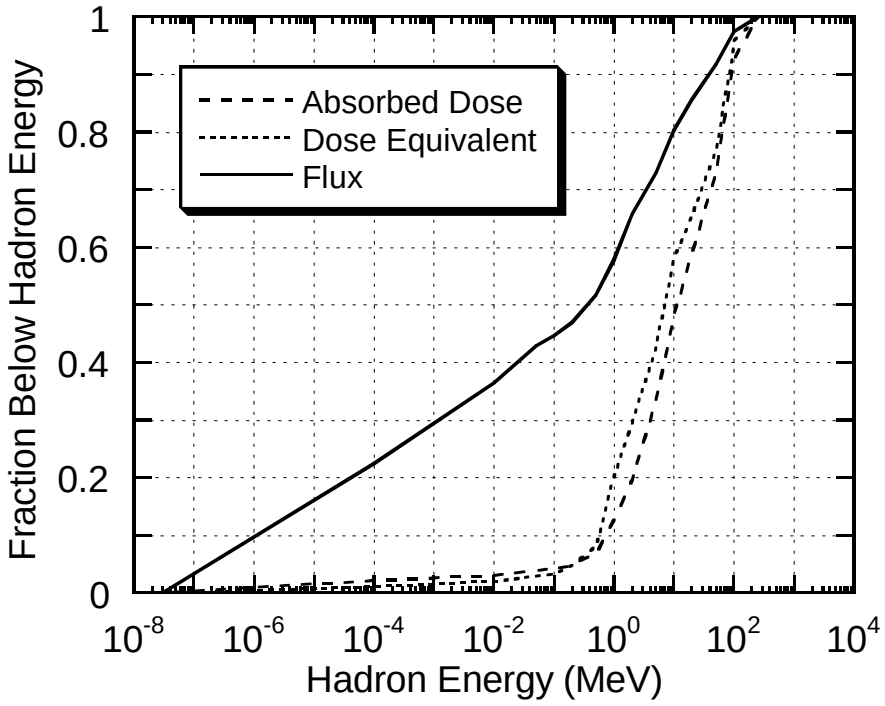

Figure 8-6:
1000 GeV/c protons incident on a solid concrete cylinder. Fraction of the omnidirectional flux, entrance absorbed dose and maximum dose equivalent below hadron kinetic energy on abscissa (in MeV) for the region between zero and 450 cm depth and between 300 cm and 750 cm radius, based on a CASIM simulation. (Fig. VI.13 of Va75.)

B) Examples of Scaling of Shielding Results

Sometimes, it is not convenient, economical or necessary to do a full Monte-Carlo calculation. In those circumstances the following prescription may be used to apply the results of an all-iron Monte-Carlo calculation to the two-media case.

1. Replace the outer layer of concrete with a thickness of iron equivalent in hadron attenuation. Roughly, 1 meter of concrete ≈ 40 cm of iron. (Since the ratio of absorption lengths = 16.8 (iron)/41.6 (concrete) = 0.4.)

2. Determine the star density at the corresponding point in the fictitious all-iron geometry.

3. Apply an appropriate radial scaling rule to compensate for the different radial distances of corresponding points in the concrete layer and its iron equivalent.

4. Use the star-to-dose conversion factors appropriate for a concrete shield (see Table 8-1).

As an example of the application of the all-iron estimate to the two media case, assume we wish to know the maximum dose rate outside a beam absorber that has iron radially to 150 cm and then concrete radially to 300 cm. The beam will be 1000 GeV/c protons with a maximum repetition rate of 10^{10} protons per pulse, once every 10 seconds. Following this prescription:

1. The outer 150 cm concrete layer is equivalent to 150 x 0.4 = 60 cm Fe.

2. The corresponding point in the fictitious all-iron geometry is 150 + 60 = 210 cm. From Fig. 8-4, the maximum star density at 210 cm in iron is 7×10^{-10} stars cm^{-3} per incident proton (at about 8 feet in the Z-coordinate downstream of the point of impact of the beam).

3. Scaling radially, we multiply by [(210 cm fictitious Fe)/(300 cm Fe + concrete)]^2 to get 3.4×10^{-10} stars cm^{-3} per incident proton for the Fe + concrete beam absorber.

4. Multiplying by the 4.9 x 10^{-3} mrem/star cm^{-3} conversion factor for thick concrete and the maximum number of protons incident per hour, 3.6 x 10^{12}, we obtain a maximum dose equivalent rate estimate of 6.0 mrem/hr.

This prescription is reliable only for a concrete layer 90 cm or thicker; thinner layers of concrete are not adequate to filter out the excess neutrons present in the iron equilibrium spectrum. It is important to note that this type of estimate is only an estimate; one should do a full Monte-Carlo calculation using MARS to obtain a more reliable value.

C) Approximate Particle Flux to Dose Equivalent Conversion Factors

Hadrons, Muons, Electrons and Photons by Energy

Figure 8-7 shows the high-energy values of dose equivalent per fluence conversion coefficients for monochromatic parallel incident particle beams (Sc90). A few general conversion factors from flux density to dose equivalent rate are provided below.

Mixture of High Energy Hadrons

Conversion of flux to dose equivalent rate for hadrons outside of a thick soil and/or concrete shield is

$$10 \text{ hadrons cm}^{-2} \text{ sec}^{-1} \cong 1 \text{ mrem-hr}^{-1}.$$

This is a reasonable approximation for an almost pure neutron leakage spectrum (St84) (that is, outside of lateral shielding). If the radiation field contains a larger charged particle component (as, e.g., in the forward direction relative to the beam) a value of

$$6.3 \text{ hadrons cm}^{-2} \text{ sec}^{-1} \cong 1 \text{ mrem-hr}^{-1} \text{ is preferred.}$$

Muons

For minimum ionizing muons (i.e., with dE/dx ≈ 2 MeV cm^2/g in tissue) conversion of flux to dose equivalent rate is

$$8.7 \text{ muons cm}^{-2} \text{ sec}^{-1} = 1 \text{ mrem-hr}^{-1}.$$

A good approximation for muons with energies between 0.1 and 100 GeV which is also widely used for muon radiation fields outside of thick shields is (St83):

$$6.9 \text{ muons cm}^{-2} \text{ sec}^{-1} = 1 \text{ mrem-hr}^{-1} \text{ (25000 muons cm}^{-2} \text{ mrem}^{-1}\text{)}.$$

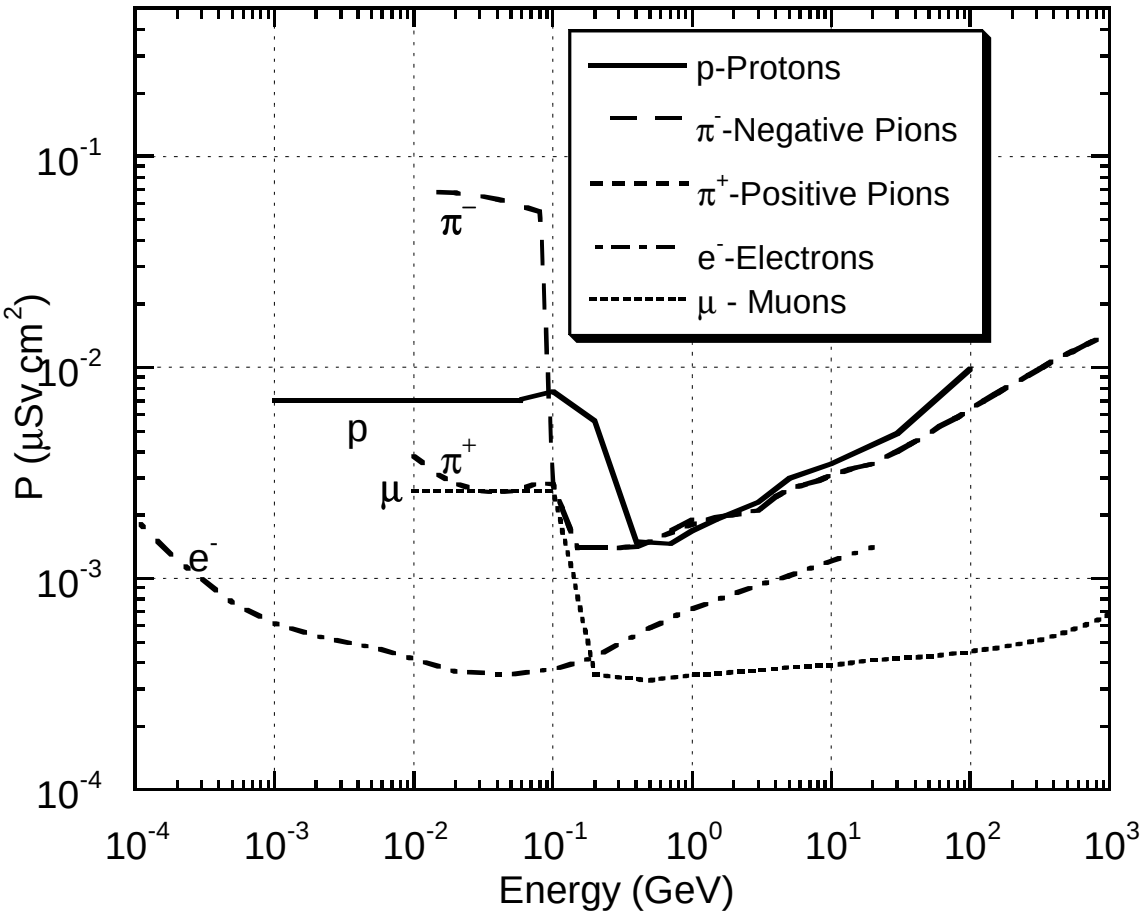

Figure 8-7 Dose equivalent per unit fluence conversion coefficients [microSv/(particle cm^{-2})] as a function of energy adapted from (Sc90). One microSievert (μSv) = 0.1 mrem.

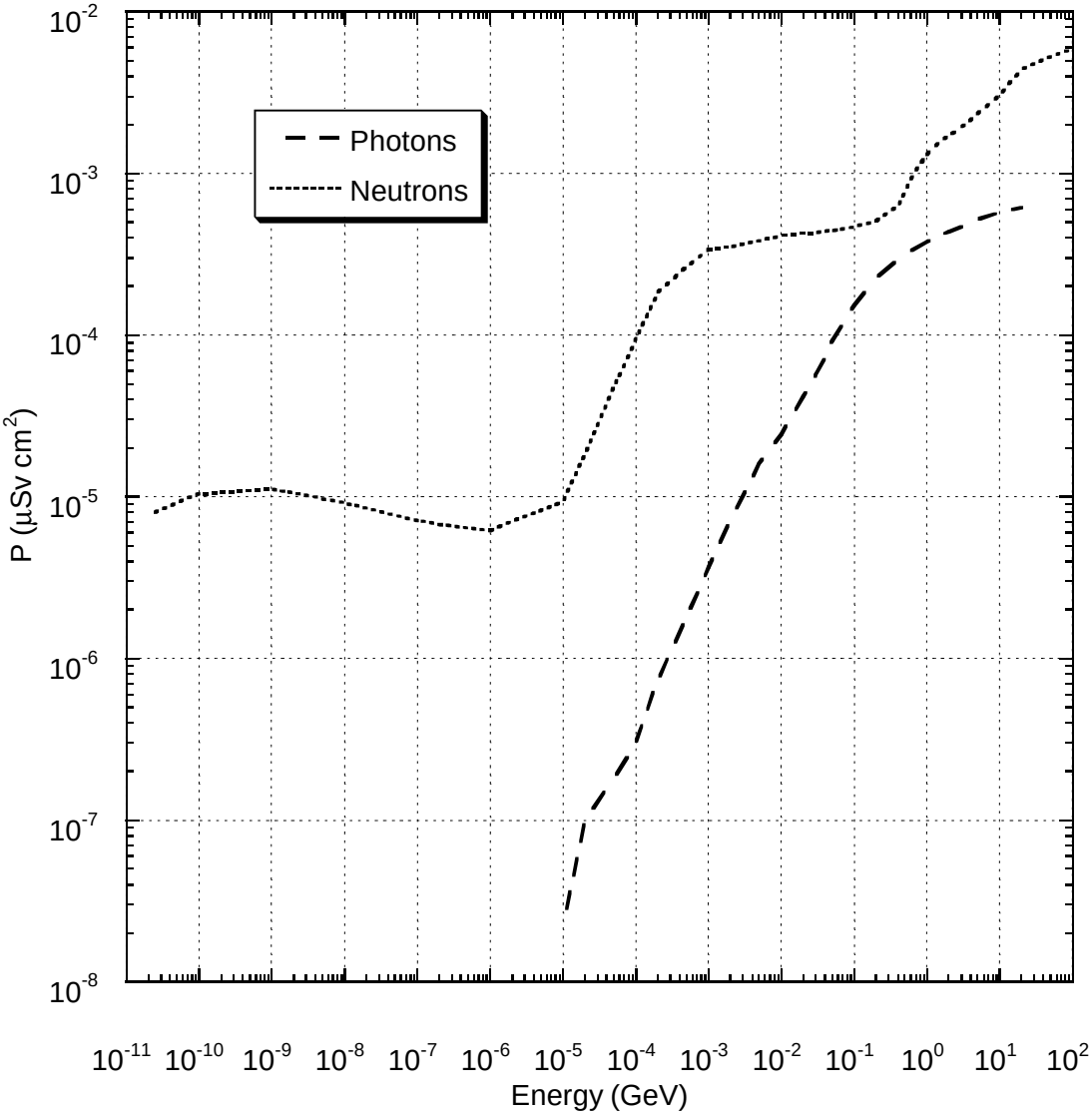

Figure 8-7 cont.

3. Prompt Radiation Shielding-Muons

A. Introduction

Energetic muons are capable of traversing large distances through matter. Their long range (e.g., ~500 m of soil for a 300 GeV muon) strongly suggests that muon shielding be treated separately from hadron shielding. The problem of estimating muon dose rates can be conveniently divided into three parts: muon production, muon transport, and beam loss mode. The first two are encoded as part of the Monte Carlo codes such as MARS or CASIM (MUSIM for muons) which trace the development of hadronic and electromagnetic showers and include muons from all generations of the showers. In a typical application, beam loss mode and geometry is user supplied and encoded. This is entirely similar to the hadron shielding case. An empirical method, suitable for rough estimates, is given by (Co99) and (Su92). As always, detailed calculations using the Monte-Carlo programs are preferred for designs of large scale shields against muons.

B. Muon Production

Muon production may be divided into (l) muons from π and K decay and (2) "prompt" muons (including those from decay of short lived particles). The π/K decay source is well understood and, when inserted into a hadronic shower simulation, reflects directly its particle production model. Prompt muons are produced in various processes by participants of the hadronic and electromagnetic showers. These processes have been included in the modern Monte-Carlo codes. At Fermilab energies the π/K decay source usually dominates.

C. Muon Transport

Muon transport is well understood and its predictions well verified at presently accessible energies. Since muons do not interact strongly their absorption cross section is negligible. They lose energy mainly through electromagnetic interactions with atomic electrons (ionization and excitation) and are Coulomb scattered by nuclei. Because of their larger mass they do not radiate as readily as do energetic electrons and not until energies reach ~100 GeV does this become an important source of energy loss. In addition to this radiation *(Bremsstrahlung)* two other processes contribute significantly to muon energy loss at high energies: direct pair production and deep inelastic scattering with nuclei. (Lo85) provides extensive tables of the average energy losses due to the various mechanisms of 1-10000 GeV muons in various materials.

Ionization losses, when measured over a short pathlength for a set of muons of the same energy, exhibit a Landau distribution that clusters narrowly around the mean energy loss though with a long "tail" due to particles which have lost a relatively large amount of energy. Where this process dominates the muon *range*

distribution tends to be an approximately Gaussian shape but again with a tail towards shorter ranges. Energy loss for the other processes aside from ionization is much more broadly distributed. This causes the muon range distribution to widen gradually with energy as these processes gain in importance. This is illustrated in (Va87) which shows the distribution of the distance of stopped muons in soil for a set of energies from 10 GeV to 20 TeV. In short, at high energies the standard deviation of the range differs little from the range or total pathlength of the muon. Thus, using the range-energy to decide how much shielding is needed to remove the muons without taking this large range straggling effect into account can lead to serious underestimates in the intensity of the muon component of the radiation field. The distinction between ionization and the other modes of energy loss is also present in the simulation where ionization is treated as a continuous process while the others are considered as individual events (except that low energy Bremsstrahlung, with $E_\gamma < 1$ MeV, is included with ionization).

In addition to losing energy while traversing bulk matter muons undergo angular diffusion. At low energies the dominant mechanism is multiple Coulomb scattering but around 1 TeV Bremsstrahlung begins to dominate. The effects of these energy-loss mechanisms are described in detail in (Va87). The validity of these models in the Fermilab energy regime is borne out by the generally good agreement between muon dose predictions and observations (Co86).

D. Beam Loss Mode

The effect of beam loss mode on dose in a typical application for muons differs considerably from the same exercise for hadrons. Consider, for example, the important case of a magnet string inside a tunnel which may represent a part of the accelerator or a beamline and where it is assumed that beam is lost at a point. For hadrons the dose outside a shield of typical dimensions is mainly due to neutrons which are relatively low in energy. Since these neutrons are unaffected by magnetic fields and have typically large production angles the results show only a relatively mild azimuthal dependence. For muons no such smearing out effects apply. Since particle energy downgrades quickly in hadronic showers the most penetrating muons will originate in the first few generations. Thus, even after long distances, effects encountered near the point of production such as from geometry or magnetic field will influence dose rate.

The π/K decay muon source in particular is quite sensitive to the geometry and hence to beam loss mode. In bulk matter its magnitude will increase (almost linearly) with the nuclear interaction length. When, as often encountered in accelerator geometries, large empty or near empty spaces are present, the π's and K's have the opportunity to decay without removal by nuclear interactions, making this component relatively more important.

Muon shielding therefore requires that one pay close attention to beam loss mode, geometry, and the presence of magnetic fields. For beam loss in an accelerator or beamline, dose generally peaks in the bend plane and this may necessitate examining the elevation of the terrain along the path of the muons for potential excursions of the muon out of the soil. The muon dose equivalent rates at the surface over large distances downstream of the protons struck by high energy protons must be examined vis-a-vis Fermilab guidelines expressed in this Manual.

4. Residual Radioactivity

A. Introduction

At all accelerators with energies greater than a few tens of MeV, induced radioactivity results whenever beams interact with accelerator or beam transport components. Typically these interactions occur at injection and extraction points and beam splitting stations. Losses at these points are not desirable, and great efforts are often required to reduce them. Beam losses also occur at collimators, scrapers, target areas and beam absorbers; these losses are deliberate and cannot be reduced. Consequently, these are usually the most radioactive areas of the accelerator, and work near them is the largest source of radiation exposure at all laboratories.

While these loss points are common to all accelerators, the magnitude of the resulting problems depends on many factors unique to each accelerator: the type of particle accelerated, the particle energy, and the geometry and composition of the items being struck. What follows is aimed primarily at practical applications at Fermilab; more general discussions may be found in (Ba69), (Go76), and (Co99).

B. Radioactivation at Proton Accelerators

The extranuclear hadron cascade process produces the major fraction of the induced radioactivity at proton accelerators. Each high-energy particle which interacts with a nucleus may be absorbed and/or knock some nucleons out of the struck nucleus, with the latter process called “spallation”. Additional high-energy particles may also be created in the collision. If the resulting nucleus is highly excited, it will de-excite by “boiling off” so-called “evaporation neutrons.” The entire nuclear reaction is called a “star” because of the many secondary particles radiating from it.

The resulting nucleus may be stable or radioactive. The cross section for producing a particular nuclide depends on the target nucleus and on the type and energy of the incident particle. These cross sections are best determined from experimental data. If such data is lacking, empirical formulae, such as that in (Ba69), give a good approximation to cross sections which vary over several orders of magnitude.

(Ba69) contains information on many cross sections which are relevant to radioactivation, and describes how to calculate induced activity levels from such data.

The particles in the cascade continue to propagate and decay or interact until their energy drops below the threshold for nuclear reactions; this is usually between 10 and 50 MeV. However, for some nuclides, neutron capture is an exoergic reaction with a large cross section for thermal neutrons. For example, the radioactivation of concrete occurs principally by thermal neutron capture of ^{23}Na to produce ^{24}Na with a 15 hour half-life.

The simple rules of thumb which follow can be used for most "back of the envelope" calculations (Go76b).

Rule 1: The exposure rate *dD/dt* (R/hr) at a distance *r* (meters) from a "point source" of gamma rays is given in terms of the source strength *S* (curies), the photon energy *E* (MeV), and the probability p_i a particular photon is emitted when the nucleus decays, by:

$$\frac{dD}{dt} = 0.4\frac{S}{r^2}\sum_i E_i p_i$$

where the summation is over all the photons emitted in the decay. The factor 0.4 is a combination of different constants and unit conversion parameters.

Rule 2: In many common materials, about 50% of the nuclear interactions produce a radionuclide with a half-life longer than a few minutes. About half of these have half-lives greater than a day.

Using these rules, we can calculate the dose rate near a target a tenth of an interaction length long. (A much longer target would require a large correction for secondary interactions.) Assume a beam of 10^{11} protons/second has struck the target for several months - long enough for many of the radionuclides produced to reach their saturation levels. Of the 10^{11} p/s incident, one tenth interact, and half of these interactions yield radionuclides of interest. The resulting decay rate is 5 x 10^9/s, or 135 mCi. (1 Curie ≡ 3.7 x 10^{10} disintegrations/second.) Assuming each decay produces a 1 MeV photon the exposure rate half a meter away shortly after beam turn off is:

$$\frac{dD}{dt} = 0.4\frac{(1\,\text{MeV})\times(0.135\,\text{Ci})}{(0.5\ \text{m})^2} = 0.245\ \text{R/hr} = 245\ \text{mR/hr}.$$

This activity will decay with time in a way which this data cannot predict, but which may be predicted reasonably well by a statistical model of Sullivan and Overton (Su65) (see Rule 3).

Rule 3: For most common shielding materials, the exposure rate due to a constant irradiation is given by:

$$\frac{dD}{dt} = B\,f \ln\left(\frac{t_i + t_c}{t_c}\right).$$

Here ϕ is the incident flux, B is a material and geometry-dependent constant, and t_i and t_c are the irradiation and cooling times, respectively. This is valid for those materials which yield many radionuclides upon irradiation and for $t_c > 12$ min, $(t_i + t_c) < 500$ days. The constant B may be determined experimentally or by using Rule 2.

Another useful rule relates the total number of stars produced by a single proton in the entire cascade to the incident proton (or hadron) energy:

Rule 4: In a cascade, a proton typically produces about four stars for each GeV of kinetic energy.

Thus a beam of 10^{12} 400 GeV p/s produces a total of 4 x 400 x 10^{12} = 1.6 x 10^{15} stars/s in its beam absorber. If 25% of the stars yield a radionuclide with a half-life greater than a day, then the total amount of moderately long-lived radioactivity in the beam absorber

$$(0.25 \text{ dis/star})\ (1.6 \text{ X } 10^{15} \text{ stars/s})/(3.7 \text{ X } 10^{10} \text{ dis s}^{-1} \text{ Ci}^{-1}) = 10.8 \text{ kCi}.$$

C. Calculational Techniques

In order to provide more accurate, and thus more useful information concerning dose rates due to activation, we must have detailed information in the following areas:

Cascade Source Term: The spatial distribution and spectra of the particles in the hadron shower in the target of interest. The accuracy of the calculation will be enhanced in accordance with the degree of detail concerning target composition and geometry that is included.

Nuclear Reaction Data: Reaction cross sections for transforming various nuclei in the "target" into other, radioactive nuclei.

Radiological Data: Nuclear lifetimes, decay schemes, transport of β's and γ's out of the activated object (i.e., self-shielding) and flux-to-dose conversion factors.

There are several calculational approaches. Monte-Carlo codes such as MARS can now adequately handle the induced radioactivity problem (Su98).

A semi-empirical approach was used by Barbier (Ba69). Barbier separates the problem into two parts: the user is given the task of determining the flux of activating particles, while Barbier provides information on residual dose rate per unit activating flux. He derives his induced spallation cross sections from an empirical formula. Experimental values of nuclear lifetimes and decay characteristics were entered into these calculations. Transport of β and γ-rays out of the material and conversion to dose rate was done in an appropriate analytic way. The results may be presented in terms of what Barbier calls the "danger parameter." This is the dose rate in a cavity inside an infinite volume of radioactive substance with uniformly distributed activity produced by unit hadron flux (1 particle/cm^2-sec). Curves of danger parameters for different materials are shown in Fig. 8-8 and are similar to conventional cooling curves. The danger parameter is a function of irradiation and cooling time, because isotopes with different lifetimes saturate and decay differently with time.

We can use one of these curves to determine the dose rate in a real situation involving a thick source by using the following relation:

$$\frac{dD}{dt} = \frac{\Omega}{4p} f \mathbf{D}.$$

The dose rate at any point, *dD/dt*, is obtained by multiplying the danger parameter (**D**) by the fractional solid angle ($\Omega/4\pi$) the source subtends when seen from the point of interest and by the activating flux density (ϕ) at the surface of the object. (The activity several absorption lengths into the body does not contribute much to the external dose rate because of self-shielding by the activated object.) An alternate representation involves the hadron star density *S* (calculated by one of the standard Monte-Carlo codes) in the activated material and a different parameter, ω. The flux and star density are related: $f = lS/r$, where λ is the interaction length expressed as mass per unit area (g cm^{-2}), and r is the density of the material (g cm^{-3}). Here, the quantities f and S include the beam intensity and are thus in units of particles cm^{-2} s^{-1} or stars cm^{-3} s^{-1}, respectively.

It is possible to obtain the hadron flux at the surface of the object from a Monte-Carlo calculation run for that purpose, or from a collection of "standard" cases. If this is done, one must be careful because many Monte-Carlo programs have a low-energy cutoff, below which they cease to follow particles. Since this

cutoff may be higher than the thresholds of many activation reactions, use of the "flux" or "star density" predicted by the Monte-Carlo calculation will give an erroneously low value for the activation. Correction for this effect may be made if the ratio of the true flux to the "Monte-Carlo flux" is known. This ratio is material dependent, and to the extent that the spectrum has not reached an equilibrium shape, it is position dependent as well.

For the 300 MeV/c ($E_n = E_p$ = 47 MeV, E_π = 190 MeV) cutoff used by Van Ginneken, the proportionality constant for iron, $\omega(t_i, t_c)$, is:

$$\omega(\infty,0) = 9 \text{ X } 10^{-6} \text{ rad hr}^{-1}/(\text{star cm}^{-3}\text{s}^{-1}), \text{ or}$$

$$\omega(30\text{d},1\text{d}) = 2.5 \text{ X } 10^{-6} \text{ rad hr}^{-1}/(\text{star cm}^{-3}\text{ s}^{-1}).$$

Curves of the danger parameter (Fig. 8-8) may be used to calculate the residual activity of various materials for different irradiation and cooling times. They may also be used for irradiation times other than the standard ones presented in the figures, as follows:

$$\frac{dD(t_i,t_c)}{dt} = \frac{dD(\infty,t_c)}{dt} - \frac{dD(\infty,t_i+t_c)}{dt} .$$

The dose rate sought is the difference between the dose rates for the case of an infinite irradiation time and two hypothetical cooling times: one equal to the actual cooling time, the other equal to the actual irradiation plus cooling times. This formula is exact.

It is far easier to make predictions of induced radioactivity than it is to verify those predictions; therefore good experimental data are scarce. The average difference between prediction and measurement is about a factor of two. Other comparisons show similar agreement, especially for relatively short irradiation times. When known cross sections and thin targets are used, the agreement is better.

D. Applications

Figure 8-9 shows a calculation of Armstrong (Ar73) to which has been added the decay curves of a number of accelerator components made mostly of iron. The curve labeled "accel" is based on the measured cooling of the average dose rate around the Fermilab Main Ring. It had been operating for 3 years with essentially constant losses; thus the curve ought to be comparable to the one labeled "one year"; but it falls about a factor of 3 below it for long cooling times.

The curve labeled "neutrino" represents the decay of an area near the target of the narrow band neutrino target train after a run of 8 months. The beam intensity

varied by a factor of about two over this period. Again, the components cooled much faster than one would predict.

Finally, the curve marked "AGS" represents the dose rate near the Brookhaven AGS slow external beam splitter. This device had been operating for many years; its decay agrees reasonably well with the predictions for long irradiations, but still falls below the prediction.

As can be seen from the various graphs of the danger parameter, different materials vary widely in their relative hazards due to activation. Aluminum is preferred to iron because of its lesser activation - the only major long-lived activity produced from aluminum is ^{22}Na. For shielding purposes, $CaCO_3$, the principal constituent of marble, is excellent for the same reason; in this case the cross section for ^{22}Na production from calcium is even lower. Elements above calcium, however, are capable of readily producing long-lived activity.

Sodium, on the other hand, is notorious for causing problems because of its high thermal neutron capture cross sections, producing ^{24}Na. Concrete containing one percent of sodium by weight produces enough ^{24}Na activity to approximately double the radiation level in the machine enclosure the first day after machine turn off. Since the major source of sodium in concrete is the aggregate, a proper choice of aggregate, such as limestone, can eliminate this problem. Evidence for the copious production of ^{56}Mn (2.6 hrs half-life) by thermal neutron capture on traces of ^{55}Mn in iron and concrete has also been observed. The neutron spectrum emanating from a thick 1 m radius iron shield was particularly rich in intermediate energy and thermal neutrons; additional thermalization occurred in the concrete. Traces of boron added to the concrete in the area would capture most of the neutrons and alleviate the problem.

The question of radioactivation of air in target and accelerator enclosures has been studied at some length. It has been a common experience, that because of the short half-lives involved (^{11}C with a half-life of 20 minutes is the longest lived apart from tritium) there is no significant internal radiation dose hazard. There is an immersion dose hazard. (Co99) describes method of estimating air activation.

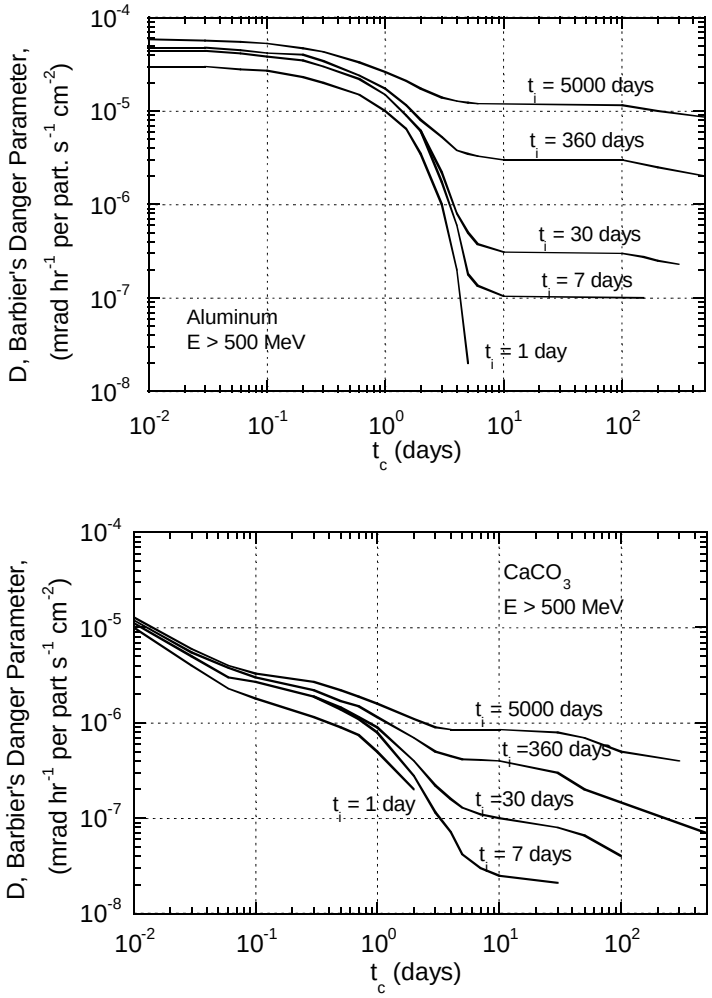

Fig. 8-8: "Danger parameter", **D**, for various materials used in accelerator construction (Ba69).

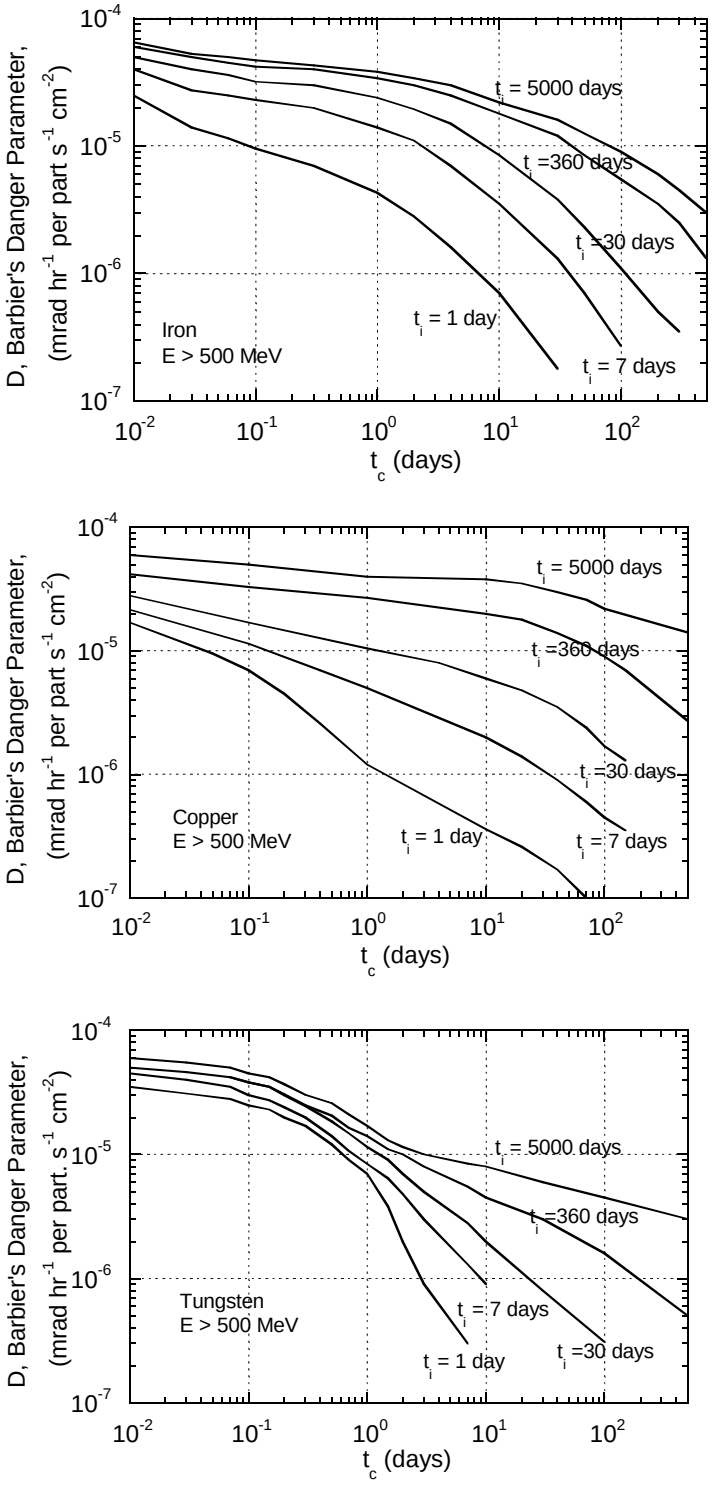

Fig. 8-8: "Danger parameter", **D**, for various materials used in accelerator construction (Ba69).

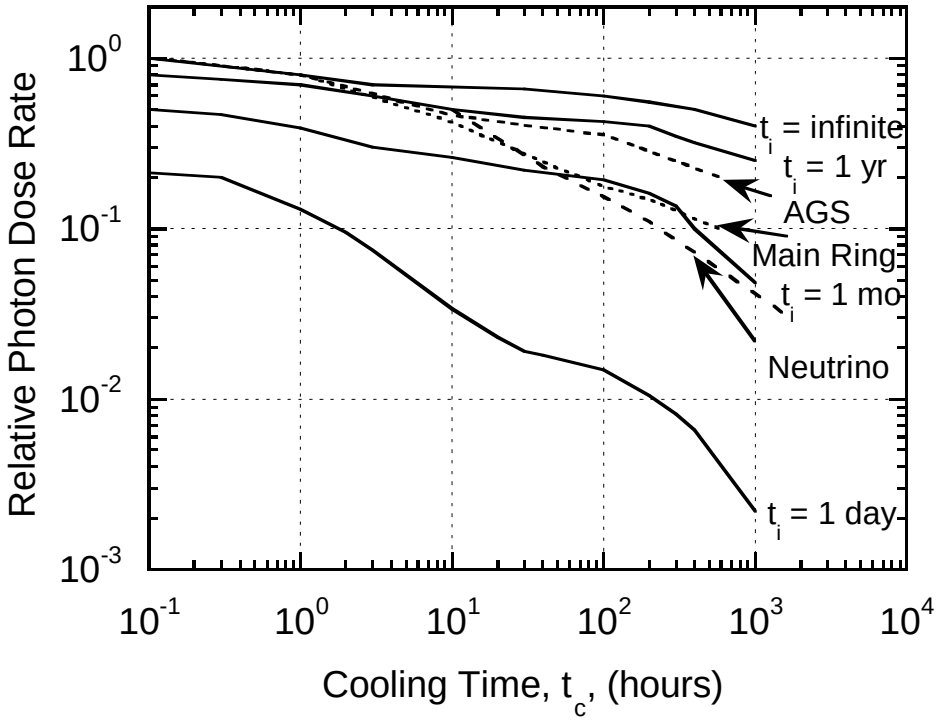

Fig. 8-9: Calculated cooling curves for various irradiation times for iron struck by high-energy protons. The curve labeled "accel" is the measured average cooling curve for the Fermilab main ring after three years of operation. The curve labeled "neutrino" is for a neutrino target train after eight months of use. The curve labeled "AGS" is for an extraction splitter in use for many years at the BNL AGS.

5. Energy Deposition

An important safety aspect of the energy dissipation of the shower is the matter of the integrity of the material wherever beam is targeted or absorbed, intentionally or not). There is the potential of melting (or vaporizing) the material. Also, when the initial energy deposition in the target is large and highly concentrated, shock waves may result which may cause the target to disintegrate — perhaps explosively. Repeated targeted beam pulses may cause target disintegration over longer time periods due to gradual deterioration of the crystalline structure. Any of these scenarios has obvious radiation (and some even conventional) safety implications. The Monte-Carlo codes are capable of predicting the density of energy deposited as a function of location in a target, which can be used to further assess the potential of radiation damage. Here electromagnetic showers must be included since, at Fermilab energies, these tend to dominate the energy deposition.

6. Low Energy Prompt Radiation Phenomena

Complex penetrations ("labyrinths") are often analyzed by means of a simple set of rules, based mostly on explicit calculations of low energy neutrons propagating through such structures (Co99, Sc90). In these calculations the source term consists exclusively of low energy neutrons, typically of a few MeV, introduced at the mouth of the labyrinth. Under such conditions these rules agree reasonably well with measurement. Likewise, the effects of neutron skyshine can also be predicted using very simple schemes (e.g., Co99, Sc90).

References

Ar73 T. W. Armstrong and R. G. Alsmiller, Jr, "Calculations of the residual photon dose rate around high energy proton accelerators", Nucl. Sci. Eng. 38 (1973) 53-62.

Aw75 M. Awschalom, P.J. Gollon, C. Moore and A. Van Ginneken, "Energy deposition in thick targets by high energy protons: measurement and calculations", Nucl. Inst. Meth. 131, (1975) 235.

Aw76 M. Awschalom, S. Baker, C. Moore, A. Van Ginneken, K. Goebel and J. Ranft, "Measurements and calculations of cascades produced by 300 GeV protons incident on a target inside a magnet", Nucl. Inst. Meth. 138 (1976) 521.

Ba69 M. Barbier, *Induced radioactivity*, (North-Holand Publishing Company, Amsterdam and London, Wiley Interscience Division, John Wiley and Sons, Inc, New York, 1969).

Co82a J.D. Cossairt, "A Collection of CASIM Calculations," TM-1140 (1982).

Co82b J.D. Cossairt, N.V. Mokhov and C.T. Murphy, "Absorbed dose measurements external to thick shielding at a high energy proton accelerator: comparison with Monte-Carlo calculations", Nucl. Inst. Meth. 197 (1982) 465.

Co85 J.D. Cossairt, S.W. Butala and M.A. Gerardi, "Absorbed dose measurements at an 800 GeV proton accelerator: comparison with Monte-Carlo calculations", Nucl. Inst. and Meth. A238 (1985) 504.

Co86 J. D. Cossairt, A. J. Elwyn, W. S. Freeman, and S. W. Butala, " A study of the transport of high energy muons through a soil shield at the Tevatron", Nucl. Inst. Meth. A276 (1986) 78-85, and J. D. Cossairt, A. J. Elwyn, and W. S. Freeman, "A study of the production and transport of muons through shielding at the Tevatron", Nucl. Inst. Meth. A276 (1986) 86-93.

Co88 J. D. Cossairt, A. J. Elwyn, W. S. Freeman, W. C. Salsbury, and P. M. Yurista, "Measurement of neutrons in enclosures and outside of shielding at the Tevatron", Fermilab-Conf-88/106 (1988) also in *Proceedings of the 22nd Midyear Meeting of the Health Physics; Topical Meeting on Instrumentation*, San Antonio, TX, December, 1988, pp. 190-199.

Co99 J. D. Cossairt, "Radiation Physics for Personnel and Environmental Protection", TM-1834, February 1999.

Co99 J. D. Cossairt, "Radiation Physics for Personnel and Environmental Protection", TM-1834, February 1999.

Eb88 F. Ebeling, R. Fohrmann, U. Otterpohl, and H.-J. Moehring, "Simulation of hadronic showers with Monte- Carlo codes at 40, 86, 300, and 1000 GeV: comparison with published measurements and first application to the design of the HERA beam dump", Particle Accelerators 23 (1988) 103-120.

El86 A. J. Elwyn and J. D. Cossairt, "A study of neutron leakage through an Fe shield at an accelerator", Health Physics 51 (1986) 723-735.

Go76a P.J. Gollon, "Dosimetry and shielding factors relevant to the design of iron beam dumps," TM-664 (1976).

Go76b P. Gollon, "Production of radioactivity by particle accelerators," TM-609 and IEEE Trans. Nucl. Sci. NS-23 (1976) 1395.

IC87 Data for use in protection against external radiation, Publication 51. Pergamon Press, Oxford, England. Further discussion of conversion factors are given by P. Gollon in Radiation Physics Note #14 (1976), and A. Elwyn in Radiation Physics Note #63 (1987). The ICRP pion values shown here at energies greater than 100 GeV are larger than those given in Stevenson's compilation which shows all hadron coefficients to be closely equal at such energies.

Kr97 O.E. Krivosheev and N.V. Mokhov, "A new MARS and its applications'", Fermilab-Conf-98/043 (1998) and SARE3 KEK Proceedings 97-5 (1997).

Lo85 W. Lohmann, R. Kopp, R. Voss, "Energy loss of muons in the energy range 1-10000GeV, CERN 85-03 (1985).

Mo86 N. V. Mokhov and J. D. Cossairt, "A short review of Monte Carlo hadronic cascade calculations in the multi-TeV energy region", Nucl. Instr. and Meth. A244 (1986) 349-355.

Mu83 C. T. Murphy, "Actual density of the neutrino berm", Fermilab RP Note 38, July 20, 1983.

Pa73 H. W. Patterson and R. H. Thomas, *Accelerator health physics,* Academic Press, new York, 1973.

Sc90 H. Schopper (editor), A. Fassò, K. Goebel, M. Höfert, J, Ranft, and G. Stevenson, *Landolt-Börnstein Numerical Data and Functional Relationships in Science and Technology New Series; Group I: Nuclear and Particle Physics Volume II: Shielding Against High Energy Radiation* (O. Madelung, Editor in Chief, Springer-Verlag, Berlin, Heidelberg, 1990).

St83 G. R. Stevenson, "Dose and Dose Equivalent from Muons", Report TIS- RP/099. CERN, Geneva, Switzerland (1983).

St84 G. R. Stevenson, "The Estimation of Dose Equivalent from the Activation of Plastic Scintillator," Health Physics 47 (1984) 837.

St86 G. R. Stevenson, "Dose equivalent per star in hadron cascade calculations", CERN Divisional Report TIS-RP/173 (1986). [Also in Schopper et al. (Sc90)].

Su65 A. H. Sullivan and T. R. Overton, "Time variation of the dose-rate from radioactivity induced in high-energy particle accelerators", Health Physics 11 (1965) 1101-1105.

Su92 A. H. Sullivan, *A guide to radiation and radioactivity levels near high energy particle accelerators* (Nuclear Technology Publishing, Ashford, Kent, United Kingdom), 1992)

Su98 T. Suzuki, M. Numajiri, S. Ban, Y. Kanda, Y, Oki, Y. Namito, T. Miura, H. Hirayama, T. Shibata, K. Kondo, M. Takasaki, K. H. Tanaka, Y. Yamanoi, M. Minakawa, H. Noumi, M. Ieiri, Y. Kato, H. Ishii, Y. Suzuki, K. Nishikawa, and N. Mokhov, "Soil shielding benchmark experiment and its simulation with MARS using secondary particles produced by 12 GeV protons", Rad. Prot. Dos. 78 (1998) 305-312.

Va75 A. Van Ginneken and M. Awschalom, "High-Energy Particle Interactions in Large Targets. I. Hadronic Cascades, Shielding, Energy Deposition" (1975), and A. Van Ginneken, FN-272 (1975).

Va87 A. Van Ginneken, P. Yurista, and C. Yamaguchi, "Shielding Calculations for Multi-TeV Hadron Colliders," Fermilab FN-447 (1987).

Yu83 P. Yurista and J.D. Cossairt, "Concrete Shielding Exterior to Iron," Fermilab TM-1024 (1983).